

Epitaxial relationship in the AlN/Si(001) heterosystem

V. Lebedev,^{a)} J. Jinschek, U. Kaiser, B. Schröter, and W. Richter
Institut für Festkörperphysik, Universität Jena, D-07743 Jena, Germany

J. Kräußlich
Institut für Optik und Quantumelektronik, Universität Jena, D-07743 Jena, Germany

(Received 19 November 1999; accepted for publication 16 February 2000)

The epitaxial growth of crystalline wurtzite AlN thin films on (001) Si substrates by plasma-assisted molecular-beam epitaxy is reported. The nucleation and the growth dynamics have been studied *in situ* by reflection high-energy electron diffraction. Cross-sectional transmission electron microscopy and x-ray diffraction investigations revealed a two-domain film structure (AlN¹ and AlN²) with a 30° rotation between neighboring domain orientations and an epitaxial orientation relationship of [0001]AlN¹||[001]Si and <01 $\bar{1}$ 0>AlN¹||< $\bar{2}$ 110>AlN²||[110]Si. A model for the nucleation and growth mechanism of 2H-AlN layers on Si(001) is proposed. © 2000 American Institute of Physics. [S0003-6951(00)03915-2]

Three common crystal structures, the wurtzite, the zincblende, and the rocksalt type are shared by the group-III nitrides.¹ Despite the potential advantages of heterostructures based on the metastable III-nitride cubic polytype, the quality of such epitaxial structures is still far away from the requirements of device applications.^{2–5} Therefore, the growth of the thermodynamically stable wurtzite phase of III nitrides^{1,2} on commonly used Si(001) substrates might be a next-best solution for the preparation of composite substrates for III-nitride electronic and optoelectronic devices. Moreover, a successful nitride film epitaxy on nominal Si(001) allows the integration of group-III-nitride optoelectronics into the well-developed Si technology.⁶

In this letter, we report on plasma-assisted molecular-beam epitaxy (PAMBE) of 2H-AlN films on Si(001) substrates. Nucleation processes and growth dynamics were studied in detail by *in situ* reflection high-energy electron diffraction (RHEED). Atomic force microscopy (AFM), cross-sectional transmission electron microscopy (XTEM), x-ray diffraction (XRD), and x-ray photoelectron diffraction (XPD) methods were used for *ex situ* characterization.

AlN films were grown in a home-made PAMBE system equipped with a radio-frequency plasma source (MPD21, Oxford Applied Research) for activated nitrogen supply. High-purity aluminum (6N5) was evaporated from a standard effusion cell. The growth rate ranged from 100 to 120 nm h⁻¹. For process monitoring, a 10 kV RHEED system was used. The growth parameters for PAMBE of high-quality 2H-AlN films were developed and optimized in earlier work on Si(111) substrates.⁷ In the present work, the optimized parameters were used to establish the growth conditions favorable for 2H-AlN film epitaxy. A model for the nucleation and growth of 2H-AlN on Si(001) was proposed, explaining the epitaxial relationship observed.

For all experiments, *p*-type (6.7 kΩ cm) nominal Si(001) (±0.5°) substrates were used without special chemical preparation. The substrates were annealed under ultra-high-

vacuum conditions at temperatures higher than 900 °C to remove the surface oxide. The surface quality was controlled by RHEED pattern observations. The annealing process was performed until obvious Kikuchi lines became clearly visible. On the clean Si(100) surface, a pronounced, streaky 2 × 1-reconstructed pattern was observed. Before the epitaxy, 1–2 ML of Al were deposited at 650 °C, leading to the transition from the 2 × 1 to the 6 × 4 surface reconstruction.⁸ The Al-induced 6 × 4 surface reconstruction was stable within the AlN nucleation temperature range.

The Al coverage seems to play a significant role, not only for preventing of an amorphous SiN_x formation on the Si surface,⁹ but also for the nucleation of AlN. The latter is evident due to the RHEED monitoring of the pregrowth surface processes, which shows that the nucleation of AlN takes place on the Al-covered Si(001) surface due to the presence of activated nitrogen in the chamber volume. Diffusing nitrogen atoms form AlN nuclei on the silicon surface underneath the Al adlayer, and after a short time (3–5 s), the Al adlayer is transformed into a noncontinuous AlN film. The RHEED pattern of the surface at the nucleation stage [Fig. 1(a)] demonstrates a superposition of 01 $\bar{1}$ 0 and $\bar{2}$ 110 reflections of the 2H-AlN lattice together with the 110 reflections of Si. The 12-fold symmetry of the RHEED pattern indicates that at the nucleation stage the AlN film consists of two types of domains (marked AlN¹ and AlN²), rotated by 30° with respect to each other. The orientation direction relationship is <01 $\bar{1}$ 0>AlN¹||< $\bar{2}$ 110>AlN²||[110]Si. From the estimation of the deposited Al volume, the thickness of these AlN domains cannot exceed 1–2 ML.

The reflexes related to Si(001) have a spotty character, indicating the rising roughness of the uncovered silicon surface during the nucleation. This finding might correspond to a strong silicon out-diffusion from the bulk substrate into the grain boundaries between adjacent AlN domains. The pronounced Si-related spots disappear after a deposition of 3–4 ML of AlN.

The subsequent epitaxy has a two-dimensional (2D) character and does not change the orientation of the domains as well as the ratio between the two domain types. This ratio

^{a)}Author to whom correspondence should be addressed; electronic mail: lvb@pinet.uni-jena.de

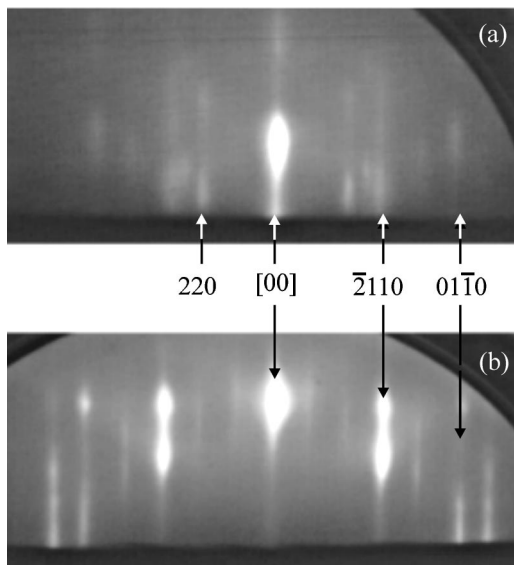


FIG. 1. RHEED observations: (a) a superimposed pattern from the Si(001) surface under AIN nucleation with a superposition of 220 Si, 01 $\bar{1}$ 0 AIN¹, and $\bar{2}$ 110 AIN² reflections; (b) 3 \times -reconstructed pattern from a 200-nm-thick AIN film surface demonstrating a superposition of the reflections from both domain types.

can be estimated from the rod intensity analysis of the RHEED pattern. For the nucleation experiments performed on nominal Si(001) substrates (unintentional miscut $\sim 0.5^\circ$), this ratio is 1:1 and does not change from the nucleation through the whole epitaxial process. Thus, we can conclude that the nucleation process determines the two-domain character of the films and the orientation of 2H-AIN domains.

The RHEED pattern from a 200-nm-thick AIN film [Fig. 1(b)] demonstrates a superposition of the reflections from both domain types. The pattern is streaky and well developed, clearly indicating a smooth surface of the epilayer. Estimated from AFM measurements, a typical value of the root-mean-square surface roughness is about 0.8 nm (200 nm AIN film). The average diameter of the domains is about 100 nm and does not depend on the growth conditions.

2H-AIN films with Al- and N-face polarity were grown as confirmed by XPD.⁷ However, the essential conditions for the formation of either the one or the other polarity of AIN epilayer on Si(001) is still under investigations.

XRD 2θ scans demonstrate the high structural perfectness of the grown films. For a 500-nm-thick AIN film, the

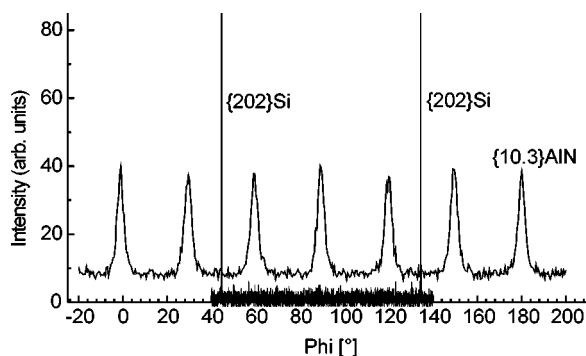


FIG. 2. XRD Φ scan demonstrates a 12-fold crystallographic symmetry of a 500-nm-thick AIN film grown on Si(001). The a_1 axis of AIN and a_1 axis of Si have a 15° angular shift.

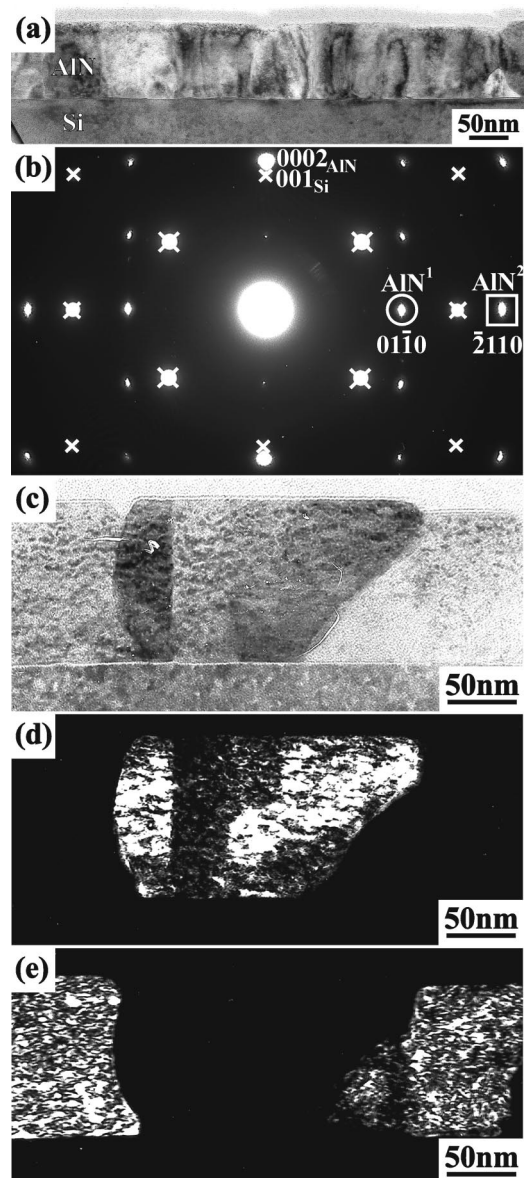


FIG. 3. (a) Bright-field XTEM image of the 2H-AIN thin film on a Si(001) substrate; and (b) diffraction pattern taken from the two-domain AIN layer (AIN¹ and AIN² reflections marked by the circle and square, respectively) and a Si substrate at the $[1\bar{1}0]$ zone axis (marked by crosses). In (c)–(e), bright- and dark-field images from the same area demonstrating the two-domain film structure. (d) corresponds to 01 $\bar{1}$ 0 AIN¹ and (e) to $\bar{2}$ 110 AIN² reflections.

full width at half maximum of the $\{0002\}$ AIN peak is 0.54° . No peaks related to the cubic phase were observed. The preferred growth direction is $[0001]$, which is parallel to the surface normal. The Φ scan (Fig. 2) demonstrates the expected 12-fold symmetry of the crystal film and the 15° lattice angle shift between $\{202\}$ Si and $\{10\bar{3}\}$ AIN diffraction peaks. The epitaxial relationship is fully in accordance with the RHEED pattern observations. The measured lattice constants for the epitaxial 2H-AIN ($a_{\text{AIN}}=0.3050$ nm, $c_{\text{AIN}}=0.4973$ nm) are slightly different from the referenced values ($a_{\text{AIN}}=0.3112$ nm, $c_{\text{AIN}}=0.4979$ nm).^{1,2}

In Fig. 3(a) a XTEM image of the AIN layer is seen in low magnification. The diffraction pattern in Fig. 3(b) was taken in Si $[1\bar{1}0]$ zone axis orientation from a region including the two AIN domain types and the Si substrate. The Si

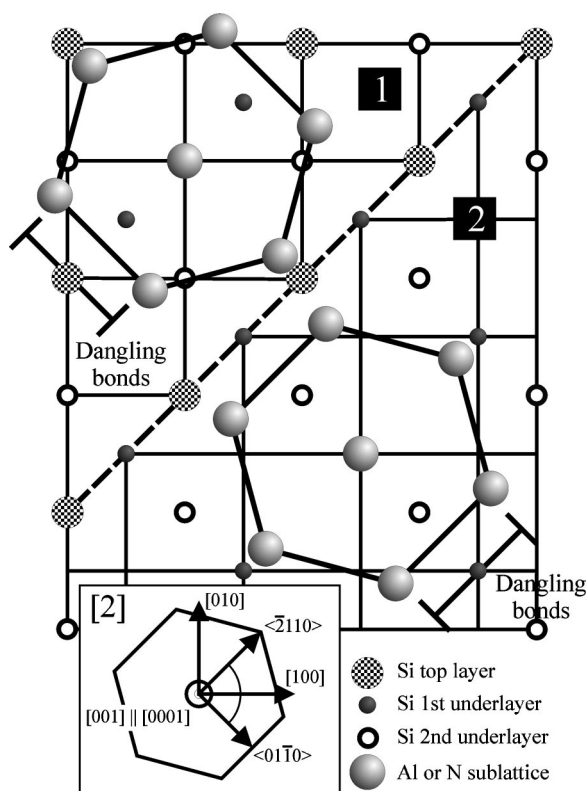


FIG. 4. Atomic arrangement for the heteroepitaxial nucleation of 2H-AlN on the Si(001) surface. The AlN nuclei with different orientations are formed on neighboring terraces (1) and (2) separated by SASB according to the Si dangling bond-directions.

reflections (indicated by crosses), domain type-1 (AlN¹ marked by a circle), and domain-type 2 (AlN² marked by a square), are seen with the orientation relationship of $[0001]\text{AlN}^1\parallel[001]\text{Si}$ and $\langle 01\bar{1}0 \rangle\text{AlN}^1\parallel\langle \bar{2}110 \rangle\text{AlN}^2\parallel[110]\text{Si}$. In Figs. 3(c)–3(e) the bright- and dark-field studies clearly demonstrate the two-domain structure of the AlN film [Fig. 3(d) was taken with the encircled reflection and Fig. 3(e) was taken with the squared reflection], and confirm the 2D character of the epitaxial process as well as the initial nucleation of both domain types as described above. Moreover, the rough Si substrate surface seen in Figs. 3(a) and 3(c) seems to agree well with the RHEED pattern observation of Si out-diffusion in the initial stage of the growth.

From the experimental results, a model for the possible heteroepitaxial nucleation and growth mechanism of 2H-AlN layers on Si(001) has been derived. According to this model, the nucleation takes place on the bulk-like plane of Si(001) under the wetting Al adlayer. It is also assumed that

on nominal Si(001) surfaces, single atomic steps dominate¹⁰ and two terrace types exist which are separated by a single atomic step boundary (SASB) (step height = $a_{\text{Si}}:4-0.1358$ nm). Terraces (1) and (2) (see Fig. 4) have a 90° angular difference between surface dangling bonds directions existing on the neighboring terraces along the $[1\bar{1}0]_1$ and $[110]_2$ directions. Thus, the nucleation of AlN¹ and AlN² nuclei on neighboring terraces with the orientation relationship to the substrate of $\langle 01\bar{1}0 \rangle\text{AlN}^1\parallel[110]\text{Si}$ and $\langle \bar{2}110 \rangle\text{AlN}^2\parallel[110]\text{Si}$ is energetically favorable due to the partial coincidence of the surface bond directions of the Si substrate and of 2H-AlN nuclei. The overall orientation relationship gives the experimentally observed 15° angle shift between $\{202\}$ Si and $\{10\bar{4}3\}$ AlN peaks (see Fig. 2) and explains the 12-fold symmetry derived from RHEED and XRD measurements.

In summary, cubic-phase-free crystalline 2H-AlN films were successfully grown by PAMBE on Si(001) substrates. The grown films have a two-domain structure with the epitaxial orientation relationship of $[0001]\text{AlN}^1\parallel[001]\text{Si}$ and $\langle 01\bar{1}0 \rangle\text{AlN}^1\parallel\langle \bar{2}110 \rangle\text{AlN}^2\parallel[110]\text{Si}$ resulting in a 12-fold crystallographic symmetry as the 2H-AlN domains are rotated by 30° with respect to each other. These findings have been confirmed by RHEED, XRD, TEM, and XPD measurements. We assume that the SASB structure of the nominal Si(001) surface determines the two-domain character of the films with nearly equivalent proportion of each domain type.

The authors would like to thank Dr. A. Fissel for stimulating discussion. This work was supported by the Deutsche Forschungsgemeinschaft (Contract No. RI 650/5-1).

¹ See, *Properties of Group III Nitrides*, edited by J. H. Edgar (INSPEC, London, 1995), Vol. 11.

² D. Gerthsen, B. Neubauer, Ch. Dieker, R. Lantier, A. Rizzi, and H. Lüth, *J. Cryst. Growth* **200**, 353 (1999).

³ D. Chandrasekhar, D. J. Smith, S. Strite, M. E. Lin, and H. Morkoç, *J. Cryst. Growth* **152**, 135 (1995).

⁴ W.-T. Lin, L.-C. Meng, G.-J. Chen, and H.-S. Liu, *Appl. Phys. Lett.* **66**, 2066 (1995).

⁵ K. Dovidenko, S. Oktyabrsky, J. Narayan, and M. Razeghi, *J. Appl. Phys.* **79**, 2439 (1996).

⁶ O. Graydon, *Opt. Laser Europe* **53**, 17 (1998).

⁷ V. Lebedev, B. Schröter, G. Kipshidze, W. Richter, *J. Comput. Phys.* **207**, 266 (1999).

⁸ C. Zhu, A. Kawazu, S. Misawa, and S. Tsukahara, *Phys. Rev. B* **59**, 9760 (1999).

⁹ U. Kaiser, P. D. Brown, I. Khodos, C. J. Humphreys, H. P. D. Schenk, and W. Richter, *J. Mater. Res.* **14**, 2036 (1999).

¹⁰ R. Fischer, H. Morkoç, D. A. Neumann, H. Zabel, C. Choi, N. Otsuka, M. Longebone, and L. P. Erickson, *J. Appl. Phys.* **60**, 1640 (1986).